

20. DATA REPORT: ISOTOPIC CHARACTERIZATION OF DISSOLVED INORGANIC CARBON IN PORE WATERS, LEG 204¹

M.E. Torres² and W.D. Rugh²

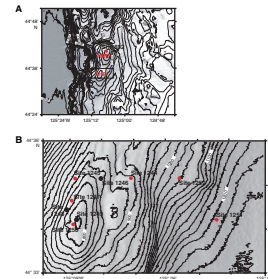
ABSTRACT

Isotopic characterization of carbon in the dissolved inorganic carbon (DIC) pool is fundamental for a wide array of scientific studies directly related to gas hydrate research. In order to generate integrated and internally consistent data of $\delta^{13}\text{C}$ of DIC in pore waters from Hydrate Ridge, we used the modern continuous flow technology of a GasBench II automated sampler interfaced to a gas source stable isotope mass spectrometer for the rapid determination (~80 samples/day) of $\delta^{13}\text{C}$ DIC in small-volume water samples. The overall precision of this technique is conservatively estimated to be better than $\pm 0.15\text{\textperthousand}$ (1σ), which is similar to the precision of methods in current use. Here we present the data generated from Ocean Drilling Program Leg 204 pore water samples.

INTRODUCTION

Drilling on Hydrate Ridge (Fig. F1) during Ocean Drilling Program (ODP) Leg 204 aimed at understanding the biogeochemical factors controlling the distribution and concentration of gas hydrates in an accretionary margin setting. Several of these objectives address fundamental questions pertaining to the carbon cycle and fluid transport in this accretionary margin in an effort to document the source and flux of hydrocarbons to the gas hydrate stability zone. The isotopic characterization of the dissolved inorganic carbon (DIC) pool is critical

F1. Hydrate Ridge bathymetry, p. 6.



¹Torres, M.E., and Rugh, W.D., 2006. Data report: Isotopic characterization of dissolved inorganic carbon in pore waters, Leg 204. In Tréhu, A.M., Bohrmann, G., Torres, M.E., and Colwell, F.S. (Eds.), *Proc. ODP, Sci. Results*, 204, 1–16 [Online]. Available from World Wide Web: <http://www-odp.tamu.edu/publications/204_SR/VOLUME/CHAPTERS/117.PDF>.

[Cited YYYY-MM-DD]

²104 COAS Administration Building, Oregon State University, Corvallis OR 97337-5503, USA. Correspondence author:

mtorres@coas.oregonstate.edu

Initial receipt: 25 February 2005

Acceptance: 19 February 2006

Web publication: 17 August 2006

Ms 204SR-117

to address these objectives, which include establishing carbon sources and metabolic paths for organic carbon decomposition ([Claypool et al.](#), this volume), as well as allowing for reconstruction of the history of the development of this gas hydrate-bearing province based on analyses of carbonate deposits.

ANALYTICAL METHOD

Traditionally, analyses of $\delta^{13}\text{C}$ of DIC in natural waters has been accomplished by either stripping the gases offline (Kroopnick, 1974) Ortiz et al., 2000) followed by injection to a mass spectrometer or by vacuum-extraction of the CO₂ by cryotrapping online with a mass spectrometer (Graber and Aharon, 1991). In addition, Salata et al. (2000) describe a method based on sample acidification and offline equilibration followed by headspace sampling and isotope measurement using a gas chromatography-combustion (GC-C) system online with a continuous-flow gas-source mass spectrometer. These methods range in analytical precision from $\pm 0.04\text{\textperthousand}$ to $\pm 0.2\text{\textperthousand}$ can be time consuming and require a minimum of 1 mL of pore water sample (see review of techniques in Torres et al., 2005).

We developed a new method for measuring $\delta^{13}\text{C}$ in DIC to allow for analysis of small volumes, which are typically available for pore water studies, while minimizing the manual labor similar to the GC-C injection method of Salata et al. (2000). The new technique, described by Torres et al. (2005), is based on direct injection of a pore water aliquot into a GasBench-II headspace autosampler, a continuous-flow interface that allows injections of several aliquots of a single gas sample into a mass spectrometer. The sample headspace is flushed automatically with helium to reduce residual air. Acid (100 μL of 43% H₃PO₄) is then injected with a gas-tight syringe and the samples are allowed to evolve DIC as CO₂ gas into the headspace. After an equilibration period of ~12 hr, the headspace gases are flushed with a helium stream, which passes through a sample loop of selected volume (50, 100, or 250 μL). The sample loop is charged with gas and a known volume of sample is then transferred to a second helium stream that flows through a gas chromatography column to separate the CO₂ from other gas compounds and a porous membrane trap to remove water. The dry sample stream is transferred to a Finnigan DELTaplusXL mass spectrometer, which integrates the relevant isotope masses (*m/z* 44, 45, and 46) as the CO₂ peak enters the source.

The method requires <0.5 mL of seawater sample (DIC > 2 mM), or ~12 μg C. For the Leg 204 pore water samples, with alkalinity values ranging from that of seawater to concentrations >100 meq/L, the sample volumes used ranged from 30 to 50 μL . This low volume requirement allowed duplicate measurements in selected samples to ascertain data precision. The technique involves little or no manual preparation of samples and allows throughput of ~80 samples per day in fully automated mode, including the delay time for equilibration. Based on multiple standard measurements, the overall precision of this technique is conservatively estimated to be better than $\pm 0.15\text{\textperthousand}$ (Torres et al., 2005). Standardization is provided by tank CO₂ referenced to an array of international standards, and analyses are monitored against a stock solution of reagent NaHCO₃.

The isotopic composition of the DIC in Leg 204 samples was measured in pore water subsamples preserved with HgCl_2 (5 $\mu\text{L/mL}$) and flame-sealed in 5-mL glass vials immediately after collection.

RESULTS

A total of 241 pore water samples were analyzed. These range from samples collected from a depositional basin, where fluid advection rate is very low (Site 1251) (Fig. F1) to the ridge summit (Sites 1248, 1249, and 1250), where rapid upward methane transport occurs (Torres et al., 2004). The isotopic data are listed in Tables T1, T2, T3, T4, T5, T6, T7, T8, and T9. The precision of the $\delta^{13}\text{C}$ measurements based on replicate analyses of a NaHCO_3 stock solution over a 7-week period was $\pm 0.08\text{\textperthousand}$.

Pore water profiles for sites at the ridge flanks and adjacent basin (Sites 1244, 1245, and 1251) (Fig. F2A, F2B) reveal the classic decrease in $\delta^{13}\text{C}$ values in the shallow subsurface resulting from oxidation of organic matter by sulfate, with minimum $\delta^{13}\text{C}$ DIC values of $-22.46\text{\textperthousand}$ (Site 1244) and $-24.86\text{\textperthousand}$ (Site 1245) coincident with the depth of sulfate depletion (Fig. F2D). These results show that although Hydrate Ridge is an area of extensive methane advection and gas hydrate formation, rapid burial of the sediments at the flanks of the ridge apparently limits the amount of methane that diffuses to the sulfate reduction zone, thus precluding a major contribution to the total DIC by anaerobic methane oxidation. This inference, based on stable isotope distributions, is supported by geochemical models based on stoichiometric sulfate and alkalinity gradients (Claypool et al., this volume), as well as by analyses of microbial activities, which at these sites show very low anaerobic methane oxidation rates (A. Boetius, pers. comm., 2004).

Upward fluid flow at the ridge summit leads to the formation of massive gas hydrate deposits in the near-surface sediments of Sites 1249 and 1250 (Tréhu, Bohrmann, Rack, Torres, et al., 2003; Tréhu et al., 2004). Pore water data are consistent with this inference, showing sulfate concentrations near zero even in the shallowest pore water samples. The $\delta^{13}\text{C}$ DIC in all fluids sampled at the summit sites is $+15\text{\textperthousand}$ (Fig. F2E, F2F), as with the fluids sampled below the sulfate reduction zone at all the other sites drilled during Leg 204. These high values reflect preferential removal of the ^{13}C -depleted DIC during methane formation (e.g., Claypool and Kaplan, 1974) such that the residual interstitial water bicarbonate shows a marked enrichment in ^{13}C . Advection of these fluids to near-surface sediments at the ridge summit results in the observed $\delta^{13}\text{C}$ DIC distribution.

In addition to characterizing the DIC sources (organic matter degradation vs. methane oxidation) and transport mechanisms (advection of deep fluids at the ridge summit), the $\delta^{13}\text{C}$ DIC in pore fluids has been incorporated into studies of carbonate phases collected during the leg to provide the framework needed to unravel the history of gas hydrate formation and destabilization recorded in benthic foraminifers and authigenic carbonate phases on Hydrate Ridge and elsewhere (Bohrmann et al., 1998; Teichert et al., 2003a, 2003b).

ACKNOWLEDGMENTS

This research used samples and/or data provided by the Ocean Drilling Program (ODP). ODP is sponsored by the U.S. National Science

T1. DIC isotope composition, Site 1244, p. 8.

T2. DIC isotope composition, Site 1245, p. 9.

T3. DIC isotope composition, Site 1246, p. 10.

T4. DIC isotope composition, Site 1247, p. 11.

T5. DIC isotope composition, Site 1248, p. 12.

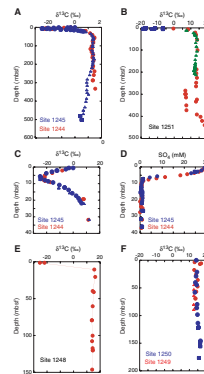
T6. DIC isotope composition, Site 1249, p. 13.

T7. DIC isotope composition, Site 1250, p. 14.

T8. DIC isotope composition, Site 1251, p. 15.

T9. DIC isotope composition, Site 1252, p. 16.

F2. Pore water DIC isotope distribution, p. 7.



Foundation (NSF) and participating countries under management of Joint Oceanographic Institutions (JOI), Inc. Funding for this research was provided by a U.S. Science Support Program postcruise research grant to M. Torres.

REFERENCES

- Bohrmann, G., Greinert, J., Suess, E., and Torres, M., 1998. Authigenic carbonates from the Cascadia subduction zone and their relation to gas hydrate stability. *Geology*, 26:647–650. doi:[10.1130/0091-7613\(1998\)026<0647:ACFTCS>2.3.CO;2](https://doi.org/10.1130/0091-7613(1998)026<0647:ACFTCS>2.3.CO;2)
- Clague, D., Maher, N., and Paull, C.K., 2001. High-resolution multibeam survey of Hydrate Ridge, offshore Oregon. In Paull, C.K., and Dillon, W.P. (Eds.), *Natural Gas Hydrates: Occurrence, Distribution, and Detection*. Geophys. Monogr., 124:297–306.
- Claypool, G.E., and Kaplan, I.R., 1974. The origin and distribution of methane in marine sediments. In Kaplan, I.R. (Ed.), *Natural Gases in Marine Sediments*: New York (Plenum), 99–139.
- Graber, E.R., and Aharon, P., 1991. An improved microextraction technique for measuring dissolved inorganic carbon (DIC), $\delta^{13}\text{C}_{\text{DIC}}$ and $\delta^{18}\text{O}_{\text{H}_2\text{O}}$ from milliliter-size water samples. *Chem. Geol.*, 94:137–144.
- Kroopnick, P., 1974. The dissolved $\text{O}_2\text{-CO}_2\text{-}^{13}\text{C}$ system in the eastern equatorial Pacific. *Deep-Sea Res., Part A*, 21:(3)169–174. doi:[10.1016/0011-7471\(74\)90059-X](https://doi.org/10.1016/0011-7471(74)90059-X)
- Ortiz, J.D., Mix, A.C., Wheeler, P.A., and Key, R.M., 2000. Anthropogenic CO_2 invasion into the northeast Pacific based on concurrent $\delta^{13}\text{C}_{\text{DIC}}$ and nutrient profiles from the California Current. *Global Biogeochem. Cycles*, 14:917–930. doi:[10.1029/1999GB001155](https://doi.org/10.1029/1999GB001155)
- Salata, G.G., Roelke, L.A., and Cifuentes, L.A., 2000. A rapid and precise method for measuring stable carbon isotope ratios of dissolved inorganic carbon. *Mar. Chem.*, 69:153–161. doi:[10.1016/S0304-4203\(99\)00102-4](https://doi.org/10.1016/S0304-4203(99)00102-4)
- Teichert, B.M.A., Bohrmann, G., Gràcia, E., Johnson, J.E., Su, X., Weinberger, J.L., and the Leg 204 Shipboard Scientific Party, 2003a. Authigenic carbonates from Hydrate Ridge (ODP Leg 204): formation processes and evidence of fluid pathways. *Geophys. Res. Abstr.*, 5:07000. (Abstract)
- Teichert, B.M.A., Eisenhauer, A., Bohrmann, G., Haase-Schramm, A., Bock, B., and Linke, P., 2003b. U/Th systematics and ages of authigenic carbonates from Hydrate Ridge, Cascadia margin: recorders of fluid flow variations. *Geochim. Cosmochim. Acta*, 67:3845–3857. doi:[10.1016/S0016-7037\(03\)00128-5](https://doi.org/10.1016/S0016-7037(03)00128-5)
- Torres, M.E., Mix, A.C., and Rugh, W.D., 2005. Precise $\delta^{13}\text{C}$ analysis of dissolved inorganic carbon in natural waters using automated headspace sampling and continuous-flow mass spectrometry. *Limnol. Oceanogr.: Methods*, 3:349–60.
- Torres, M.E., Wallmann, K., Tréhu, A.M., Bohrmann, G., Borowski, W.S., and Tomaru, H., 2004. Gas hydrate growth, methane transport, and chloride enrichment at the southern summit of Hydrate Ridge, Cascadia margin off Oregon. *Earth Planet. Sci. Lett.*, 226:225–241. doi:[10.1016/j.epsl.2004.07.029](https://doi.org/10.1016/j.epsl.2004.07.029)
- Tréhu, A.M., Long, P.E., Torres, M.E., Bohrmann, G., Rack, F.R., Collett, T.S., Goldberg, D.S., Milkov, A.V., Riedel, M., Schultheiss, P., Bangs, N.L., Barr, S.R., Borowski, W.S., Claypool, G.E., Delwiche, M.E., Dickens, G.R., Gracia, E., Guerin, G., Holland, M., Johnson, J.E., Lee, Y.-J., Liu, C.-S., Su, X., Teichert, B., Tomaru, H., Vanneste, M., Watanabe, M., and Weinberger, J.L., 2004. Three-dimensional distribution of gas hydrate beneath southern Hydrate Ridge: constraints from ODP Leg 204. *Earth Planet. Sci. Lett.*, 222(3–4):845–862. doi:[10.1016/j.epsl.2004.03.035](https://doi.org/10.1016/j.epsl.2004.03.035)
- Tréhu, A.M., Bohrmann, G., Rack, F.R., Torres, M.E., et al., 2003. *Proc. ODP, Init. Repts.*, 204 [Online]. Available from World Wide Web: <http://www-odp.tamu.edu/publications/204_IR/204ir.htm>. [Cited 2005-02-25]

Figure F1. A. Bathymetry of the Hydrate Ridge region. Box shows location of southern Hydrate Ridge (SHR) and ODP Site 892 on northern Hydrate Ridge (NHR). B. Detailed topography of SHR area targeted by Leg 204. Bathymetry from Clague et al. (2001).

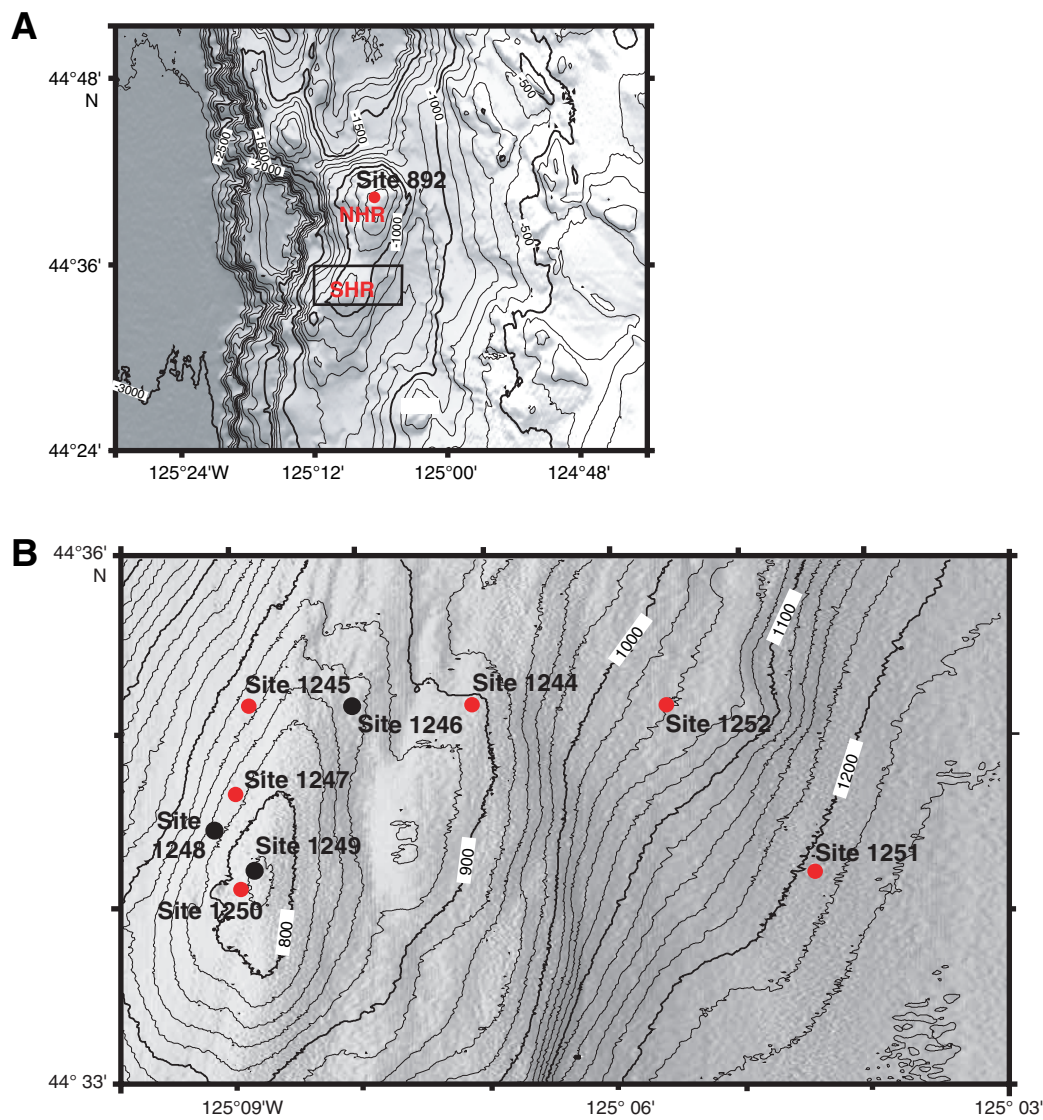


Figure F2. Downcore distribution of $\delta^{13}\text{C}$ DIC in pore waters from southern Hydrate Ridge (SHR). A. Fluids sampled at Sites 1244 and 1245. Symbols denote different holes at each site. B. Fluids from Site 1251, drilled at a depositional basin east of SHR. Symbols denote samples from different holes drilled at this site and are in excellent agreement with data collected among the three holes. C. $\delta^{13}\text{C}$ depletion in upper 10 mbsf at Sites 1244 and 1245. Corresponds to the depth of sulfate depletion illustrated in D. D. Sulfate depletion at Sites 1244 and 1245 (Tréhu, Bohrmann, Rack, Torres, et al., 2003). E. Fluids from Site 1248 in which vertical advection brings ^{13}C -enriched fluids to shallow depths consistent with inferences made on other pore water data (Tréhu, Bohrmann, Rack, Torres, et al., 2003). Advection is most pronounced at the summit Sites 1250 and 1249, where heavy DIC is observed even in the shallowest samples, which are also depleted in sulfate, as illustrated in F. F. Sulfate depletion at Sites 1249 and 1250 (Tréhu, Bohrmann, Rack, Torres, et al., 2003).

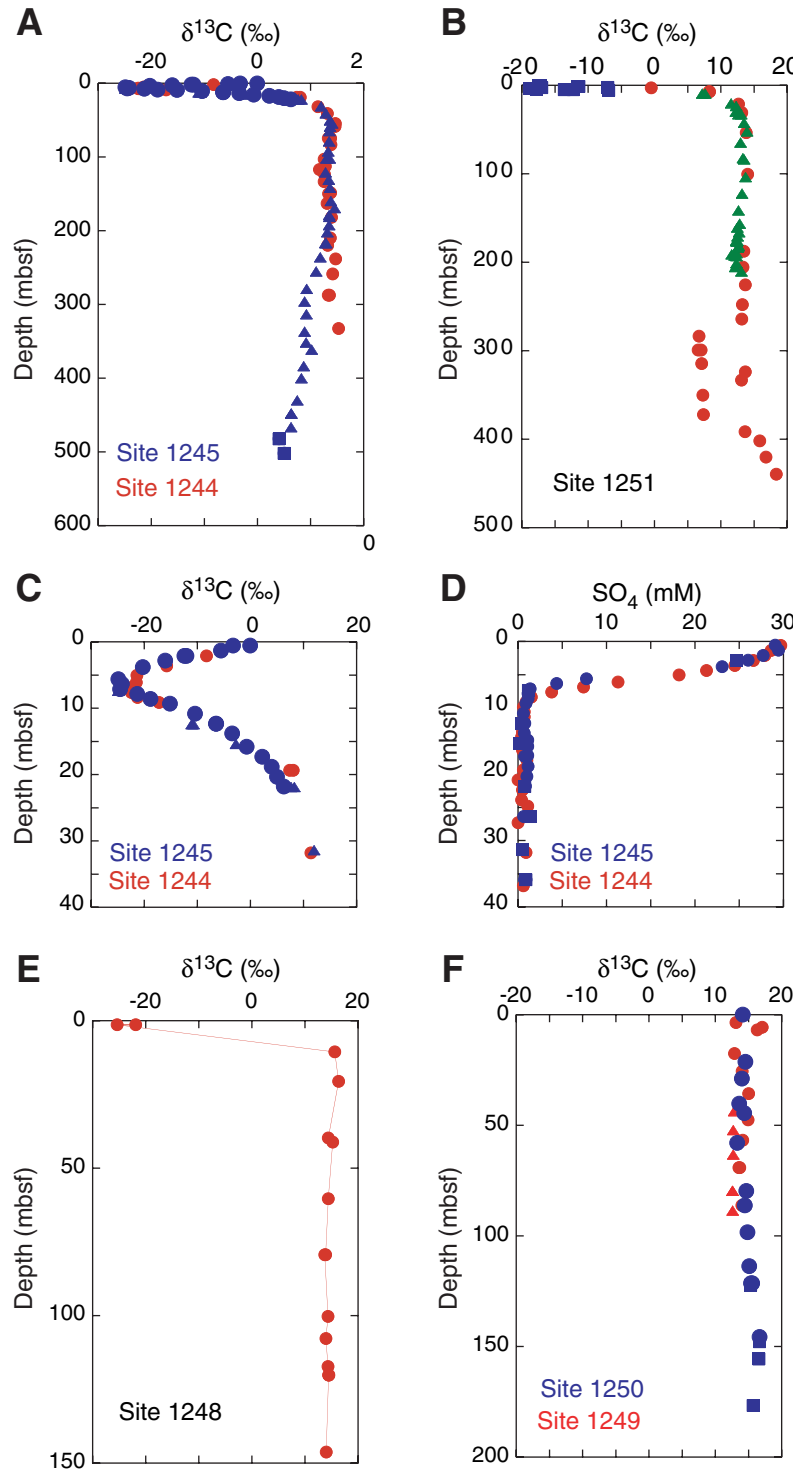


Table T1. Dissolved inorganic carbon isotopic composition in pore fluid samples, Site 1244.

Core, section, interval (cm)	Depth (mbsf)	$\delta^{13}\text{C}$ PDB (‰)
204-1244C-		
1H-1, 65–75	0.65	-3.14
1H-1, 65–75	0.65	-3.22
1H-2, 65–75	2.15	-8.28
1H-3, 65–75	3.65	-15.74
1H-4, 60–70	5.10	-21.41
2H-1, 65–75	6.15	-21.49
2H-1, 140–175	6.90	-22.46
2H-2, 66–75	7.65	-22.21
2H-2, 140–175	7.65	-22.46
2H-2, 140–175	8.40	-21.27
2H-3, 65–75	9.15	-17.23
3H-3, 140–150	19.40	8.06
3H-3, 140–150	19.40	7.39
4H-5, 135–150	31.85	11.43
5H-5, 135–150	41.35	13.18
7H-2, 135–150	54.79	14.67
7H-5, 135–150	58.97	14.61
9H-2, 135–150	74.85	13.77
9H-2, 135–150	74.85	13.37
10H-2, 55–70	83.55	13.82
12H-2, 135–150	103.35	12.58
13H-2, 135–150	112.85	12.78
13H-5, 135–150	117.35	11.68
15H-2, 135–150	123.85	12.65
17H-2, 30–45	133.70	12.59
19X-5, 140–150	149.85	13.41
19X-5, 140–150	148.85	13.79
21X-3, 135–150	163.15	13.13
23X-3, 140–150	182.25	13.93
26X-3, 135–150	210.10	13.72
27X-3, 130–150	220.10	13.21
29X-3, 140–150	238.56	14.72
31X-3, 135–150	258.65	14.20
34X-3, 130–150	287.60	13.33
34X-3, 130–150	287.60	13.54
29X-1, 130–150	332.80	15.28

Note: PDB = PeeDee belemnite.

Table T2. Dissolved inorganic carbon isotopic composition in pore fluid samples, Site 1245.

Core, section, interval (cm)	Depth (mbsf)	$\delta^{13}\text{C}$ PDB (‰)	Core, section, interval (cm)	Depth (mbsf)	$\delta^{13}\text{C}$ PDB (‰)			
204-1245B-								
1H-2, 140–150	2.9	-15.93	41X-2, 125–150	361.25	10.22			
1H-5, 140–150	7.4	-24.86	43X-4, 125–150	383.55	8.75			
2H-2, 140–150	12.4	-11.07	45X-2, 125–150	399.85	8.26			
2H-2, 140–150	12.4	-10.74	49X-4, 0–25	430.11	7.5			
2H-2, 140–150	15.4	-2.72	51X-2, 125–150	447.95	6.35			
3H-2, 140–150	21.9	7.66	51X-2, 125–150	447.95	6.42			
3H-2, 140–150	21.9	8.32	53X-2, 125–150	466.51	6.34			
4H-2, 140–150	31.4	12	204-1245D-					
5H-2, 140–150	40.9	12.92	1H-1, 60–70	0.6	-3.28			
6H-2, 140–150	50.4	13.65	1H-1, 135–150	1.35	-5.54			
6H-5, 78–88	54.28	14.05	1H-2, 65–76	2.15	-12.46			
7H-2, 140–150	58.95	13.67	1H-2, 65–76	2.15	-12.07			
8H-2, 132–142	64.99	13.6	1H-2, 135–150	2.85	-16.03			
9H-2, 134–144	78.66	13.5	1H-3, 85–100	3.85	-20.26			
10H-5, 140–150	92.53	13.37	2H-1, 65–75	5.65	-24.86			
11H-5, 140–150	101.87	13.64	2H-1, 135–150	6.35	-24.22			
11H-5, 140–150	101.87	13.03	2H-2, 65–75	7.15	-24.55			
13H-5, 104–119	120.8	12.83	2H-2, 135–150	7.85	-21.3			
15X-3, 130–150	130.66	13.46	2H-3, 65–75	8.65	-18.82			
16X-3, 130–150	141.8	13.69	2H-3, 135–150	9.35	-15.17			
19X-2, 125–150	159.75	13.83	2H-4, 135–150	10.85	-10.41			
20X-2, 125–150	169.25	14.53	2H-5, 135–150	12.35	-6.47			
21X-2, 117–142	178.77	13.49	2H-5, 135–150	12.35	-6.43			
21X-4, 77–102	181.27	13.58	2H-6, 135–150	13.85	-3.42			
22X-5, 125–150	192.65	13.52	3H-1, 135–150	15.85	-0.71			
23X-5, 125–150	201.95	13.16	3H-2, 135–150	17.35	2.23			
25X-2, 125–150	216.74	12.95	3H-3, 135–150	18.85	4.02			
25X-2, 125–150	216.74	12.8	3H-4, 135–150	20.35	5			
27X-2, 125–150	236.05	11.85	3H-5, 135–150	21.85	6.29			
29X-2, 125–150	255.35	11.05	204-1245E-					
31X-5, 125–150	278.76	9.29	2R-1, 69–89	482.29	4.09			
34X-2, 125–150	295.95	8.92	4R-1, 130–150	502.2	5.01			
36X-2, 125–150	313.15	9.24	4R-1, 130–150	502.2	5.13			
38X-5, 125–150	336.95	8.91						
40X-2, 125–150	351.65	9.2						

Note: PDB = PeeDee belemnite.

Table T3. Dissolved inorganic carbon isotopic composition in pore fluid samples, Site 1246.

Core, section, interval (cm)	Depth (mbsf)	$\delta^{13}\text{C}$ PDB (‰)
204-1246B-		
1H-2, 145–150	2.95	-10.13
2H-2, 145–160	7.65	-30.25
2H-5, 145–150	12.15	-11.62
3H-2, 140–150	17.1	2.35
5H-2, 140–150	36.1	9.52
7H-2, 130–140	54.89	11.67
9H-2, 140–150	73.81	13.49
11H-2, 140–150	93.1	14.35
11H-2, 140–150	93.10	14.14
13H-2, 135–150	112.05	13.96
16H-2, 140–150	132.70	14.29

Note: PDB = PeeDee belemnite.

Table T4. Dissolved inorganic carbon isotopic composition in pore fluid samples, Site 1247.

Core, section, interval (cm)	Depth (mbsf)	$\delta^{13}\text{C}$ PDB (‰)
204-1247B-		
1H-1, 140-150	1.40	-3.32
2H-1, 140-150	5.00	-11.86
2H-2, 140-150	6.50	-17.16
2H-3, 140-150	8.00	-19.60
2H-5, 140-150	11.00	-19.52
2H-5, 140-150	11.00	-19.34
2H-6, 140-150	12.50	-13.54
2H-7, 77-78	13.37	-9.60
3H-2, 140-150	16.00	-0.50
6H-2, 140-150	37.00	12.06
8H-2, 140-150	56.00	13.39
8H-2, 140-150	56.00	13.84
10H-5, 140-150	79.50	13.34
12H-5, 40-150	97.51	12.01
15X-2, 135-150	116.45	14.37
19X-2, 127-147	137.37	13.15
21X-3, 130-150	158.20	14.33
25X-3, 130-151	196.33	12.08
27X-3, 130-151	215.50	10.78

Note: PDB = PeeDee belemnite.

Table T5. Dissolved inorganic carbon isotopic composition in pore fluid samples, Site 1248.

Core, section, interval (cm)	Depth (mbsf)	$\delta^{13}\text{C}$ PDB (‰)
204-1248C-		
1H-1, 0–20	0.0	-18.54
1H-1, 0–20	0.0	-19.96
1H-2, 0–20	1.20	-0.93
2H-1, 77–87	7.27	17.60
2H-3, 91–101	9.16	17.99
204-1248C-		
1X-1, 138–148	1.38	-25.37
2X-CC, 0–15	10.68	15.62
3X-1, 140–150	20.60	16.33
5X-1, 140–150	39.80	14.40
5X-CC, 18–28	41.18	15.23
7H-2, 140–150	60.40	14.41
9H-2, 130–150	79.40	13.89
9H-2, 130–150	79.40	13.73
11H-4, 122–137	100.36	14.32
12H-2, 131–146	107.81	13.97
13H-2, 135–150	117.33	14.37
13H-4, 132–147	120.21	14.50
13H-4, 132–147	120.21	14.46
17X-3, 135–150	146.35	14.01

Note: PDB = PeeDee belemnite.

Table T6. Dissolved inorganic carbon isotopic composition in pore fluid samples, Site 1249.

Core, section, interval (cm)	Depth (mbsf)	$\delta^{13}\text{C}$ PDB (‰)
204-1249C-		
2H-2, 15–30	3.55	13.11
3H-1, 74–89	5.74	17.07
3H-1, 41–51	6.96	16.33
4H-5, 86–101	17.61	12.91
5H-2, 20–25	25.70	14.04
7H-1, 71–86	35.71	15.01
8H-3, 18–33	47.64	14.94
9H-2, 133–148	56.83	14.14
11H3, 104–119	69.17	13.57
11H-3, 104–119	69.17	13.71
13H-2, 79–99	86.29	14.00
204-1249F-		
9H-3, 140–150	43.61	12.87
10H-2, 140–150	52.09	12.73
12H-2, 131–146	63.20	12.73
15H-5, 135–150	79.57	12.64
15H-5, 135–150	79.57	12.58
16H-4, 135–150	88.50	12.64

Note: PDB = PeeDee belemnite.

Table T7. Dissolved inorganic carbon isotopic composition in pore fluid samples, Site 1250.

Core, section, interval (cm)	Depth (mbsf)	$\delta^{13}\text{C}$ PDB (‰)
204-11250C-		
1H-1, 0–10	0.00	14.14
3H-5, 140–150	21.40	14.55
4H-4, 140–150	29.00	13.99
5H-5, 133–143	40.31	13.61
6H-2, 47–67	44.57	14.37
7H-5, 130–140	58.00	13.29
10H-5, 135–150	79.80	14.65
11H-3, 95–110	86.36	14.44
12H-5, 140–155	98.43	14.85
14H-2, 130–150	113.80	15.12
15H-1, 106–126	121.56	15.56
15H-1, 106–126	121.56	15.39
19X-5, 130–150	145.75	16.65
204-1250F-		
5H-1, 130–150	122.30	15.33
10X-3, 130–150	147.90	16.68
11X-2, 98–123	155.68	16.58
11X-2, 98–123	155.68	16.56
13X-3, 125–150	176.65	15.71

Note: PDB = PeeDee belemnite.

Table T8. Dissolved inorganic carbon isotopic composition in pore fluid samples, Site 1251.

Core, section, interval (cm)	Depth (mbsf)	$\delta^{13}\text{C}$ PDB (‰)	Core, section, interval (cm)	Depth (mbsf)	$\delta^{13}\text{C}$ PDB (‰)
204-1251B-					
1H-2, 145–150	2.95	-0.46	11H-4, 0–15	82.29	13.36
1H-5, 145–150	7.45	8.22	11H-4, 135–150	83.64	13.51
1H-5, 145–150	7.45	8.32	13H-6, 0–20	103.67	13.74
3H-2, 145–150	21.43	12.67	15H-5, 0–15	122.40	13.21
4H-2, 145–150	31.00	13.18	17H-5, 0–15	141.40	12.66
6H-5, 131–141	53.61	13.82	17H-5, 0–15	141.40	12.68
11H-5, 70–90	100.74	14.03	19H-2, 130–150	156.31	12.85
23H-4, 102–122	187.72	13.47	19H-5, 130–150	160.81	12.49
26X-2, 130–150	205.83	13.35	20H-2, 125–150	166.13	12.77
28X-2, 125–150	225.85	13.69	20H-5, 125–150	170.63	12.55
30X-4, 110–135	248.00	13.28	22X-1, 20–40	175.60	12.51
32X-2, 125–150	264.45	13.17	22X-1, 20–40	175.60	12.29
34X-2, 128–148	283.78	6.72	22X-2, 0–20	176.87	12.40
36X-5, 80–100	299.40	7.02	23X-2, 122–147	181.82	12.72
36X-5, 80–100	299.40	6.58	23X-3, 125–150	183.32	12.56
38X-3, 130–150	314.60	7.13	24X-2, 0–25	189.62	12.38
39X-3, 130–150	324.20	13.72	24X-3, 0–10	191.12	11.66
41X-2, 130–150	333.40	13.12	24X-3, 140–150	192.52	12.12
43X-2, 130–150	350.43	7.28	24X-4, 43–63	193.05	12.38
45X-3, 130–150	372.30	7.38	25X-2, 125–150	200.95	12.35
47X-3, 130–150	391.60	13.66	25X-2, 125–150	205.45	12.18
49X-3, 130–150	402.20	15.88	26X-3, 125–150	210.38	13.11
51X-3, 130–150	420.50	16.81			
53X-3, 130–150	439.78	18.37			
204-1251D-					
1X-1, 140–150	1.40	-17.39	204-1251E-		
1X-2, 90–100	2.40	-17.41	1H-1, 85–95	0.85	-17.40
2X-1, 140–150	9.50	7.19	1H-1, 85–95	0.85	-17.25
2X-1, 50–60	9.50	7.65	1H-1, 140–150	1.40	-11.57
3X-2, 140–150	20.50	11.58	1H-1, 140–150	1.40	-11.39
3X-4, 140–150	23.50	12.34	1H-2, 80–90	2.30	-7.03
4H-2, 140–150	29.80	12.28	1H-2, 140–150	2.90	-16.96
4H-2, 140–150	32.80	13.05	1H-3, 60–70	3.60	-18.81
4H-2, 140–150	32.80	12.68	1H-3, 140–150	4.40	-17.81
5H-5, 0–10	42.40	13.52	1H-4, 60–70	5.10	-12.22
7H-3, 135–150	52.07	13.95	1H-4, 60–70	5.10	-13.58
8H-5, 135–150	64.75	13.00	1H-4, 140–150	5.90	-6.89

Note: PDB = PeeDee belemnite.

Table T9. Dissolved inorganic carbon isotopic composition in pore fluid samples, Site 1252.

Core, section, interval (cm)	Depth (mbsf)	$\delta^{13}\text{C}$ PDB (‰)
204-1252A-		
1H-1, 135–150	1.35	9.93
1H-2, 130–150	2.85	-17.72
1H-3, 85–100	3.85	-17.43
2H-1, 135–150	6.25	-10.32
2H-2, 135–150	7.75	-1.10
2H-3, 135–150	9.25	-2.2
2H-4, 135–150	10.75	4.10
2H-4, 135–150	10.75	4.45
2H-5, 135–150	12.25	0.76
2H-6, 135–150	13.75	1.99
3H-2, 135–150	16.00	4.63
8H-2, 135–150	64.75	8.57
10H-2, 45–60	82.85	8.20
12H-2, 135–150	102.75	6.84
12H-2, 135–150	102.75	6.76
14H-2, 135–150	121.75	9.64
16X-4, 130–150	140.50	11.76
16X-4, 130–150	140.50	9.47
20X-3, 130–150	177.80	14.66
22X-3, 130–150	197.00	14.29
24X-3, 130–150	215.50	14.18
26X-3, 130–150	234.80	-1.98
26X-3, 130–150	234.80	-2.22

Note: PDB = PeeDee belemnite.